Chemical Engineering Journal 84 (2001) 315–320

Chemical Engineering Journal

www.elsevier.com/locate/cej

The effect of gravity on relative contributions of natural and Marangoni convections in a liquid bridge

Yasunori Okano [a,*,1], Nicholas Audet [a], Sadik Dost [a], Sei-ichi Kunikata [b]

[a] Department of Mechanical Engineering, University of Victoria, Victoria, BC, Canada V8W 3P6

[b] Department of Materials Science and Chemical Engineering, Shizuoka University, Johoku 3-5-1, Hamamatsu 432-8561, Japan

Received 19 July 2000; received in revised form 8 November 2000; accepted 15 November 2000

Abstract

Two-dimensional laminar natural and Marangoni convection modes in a full-zone liquid bridge have been studied numerically using the control volume method with SIMPLE algorithm. The maximum Reynolds number was described as follows: in the Marangoni convection dominant regime, $Re_{\max} = 0.0405 BiMa$ ($Re_{\max}Pr < 1$) and $Re_{\max} = 0.15\{(BiMa)^2/Pr\}^{1/3}$ ($Re_{\max}Pr > 1$). In the natural convection dominant regime, $Re_{\max} = 2.61 \times 10^{-3}\, BiGr$ ($Re_{\max}Pr < 1$) and $Re_{\max} = 0.0831(BiGr/Pr\}^{1/2}$ ($Re_{\max}Pr > 1$). Graphical representations are proposed for the purpose of determining the relative contributions of these two convection modes in the liquid bridge. The transition between the natural and Marangoni convection dominant regimes occurs at around $(Ma/Gr) = 10^{-1}$ ($Re_{\max}Pr < 1$) and $(Ma^4PrBi/Gr^3) = 1$ ($Re_{\max}Pr > 1$). It was shown that the transient behavior of natural convection under varying gravity fields depends on the physical properties of the liquid. In order to reach a steady-state convection regime, a period of time is required after the stabilization of the gravity field.

Keywords: Marangoni convection; Natural convection; Liquid bridge

1. Introduction

Bulk single crystals of semiconductors and oxides are essential materials for most electronic and optoelectronic devices. These bulk single crystalline materials are obtained by a process called “crystal growth from melt”. Czochralski (CZ), Vertical Bridgman (VB), and the floating-zone (FZ) [1] are among the techniques used to grow bulk high quality crystals. Each of these techniques has some advantages and disadvantages over the others. For instance, CZ and VB allow the growth of large bulk crystals, but since the growth is achieved in a container called “crucible”, the contamination from the crucible to grown crystals represents a major setback for some materials (such as silicon with low oxygen concentration). The growth in FZ, however, is achieved in a containerless environment (i.e. without a crucible). The problem of crucible contamination is thus no issue. This is the main advantage of FZ over other bulk growth techniques.

In the floating-zone technique, the selected material in the form of a rod is placed in a furnace. A section of the rod is then heated externally until it melts. The melted section is suspended as a liquid bridge which has a free surface with its environment. This melted zone is called the liquid floating zone, or molten zone, or liquid bridge. When the rod moves upward relative to the heater, the upper section of the rod melts (since it gets hotter) and at the same time the lower section of the liquid bridge freezes (since it gets cooler). When this process continues, a section of the rod becomes newly grown single crystal material. The melting section of the rod is called feeding material, and the freezing section is called grown crystal.

During the FZ growth process, large temperature gradients cause two types of well-known convective flows in the molten zone: (i) the buoyancy-driven natural convection due to density differences, and (ii) the Marangoni convection due to the surface tension gradient. Relative importance of these convective flows depends on the growth technique considered. For instance, in CZ and VB the Marangoni convection either does not exist or is very small compared with the natural convection. In the floating-zone technique, on the other hand, the Marangoni convection may become more pronounced due to the relatively small volume of the liquid bridge even under normal gravity conditions. For instance, a typical size of molten zone used in silicon growth experiments on Earth is 1 cm in height and 1 cm in

* Corresponding author. Tel.: +81-53-478-1169; fax: +81-53-478-1169.
E-mail address: tcyokan@ipc.shizuoka.ac.jp (Y. Okano).

[1] On leave from the Department of Materials Science and Chemical Engineering, Shizuoka University, Japan.

1385-8947/01/$ – see front matter
PII: S1385-8947(00)00377-6

Nomenclature

Asp	aspect ratio (L/R)
Bi	Biot number (hL/κ)
g	gravitational acceleration (m/s^2)
Gr	$g\beta(T_{\rm p}-T_{\rm m})L^3/\nu^2$
h	heat transfer coefficient (J/(m^2 s K))
L	distance between upper and lower rods (m)
Ma	Marangoni number ($\lvert\partial a/\partial T^*\rvert(T_{\rm p}-T_{\rm m})L/(\nu\mu)$)
p	dimensionless pressure ($p^*/(\rho\nu^2/R^2)$)
Pr	Prandtl number (ν/α)
r	dimensionless radial coordinate (r^*/R)
R	radius of liquid bridge (m)
Re	Reynolds number (u^*L/ν)
t	dimensionless time ($t^*/(R^2/\nu)$)
T	dimensionless temperature ($(T^*-T_{\rm m})/(T_{\rm p}-T_{\rm m})$)
$T_{\rm a}$	ambient gas temperature (K)
$T_{\rm m}$	temperature of liquid/solid interface (K)
$T_{\rm p}$	peak temperature in ambient (K)
u	dimensionless velocity in axial direction (u^*R/ν)
v	dimensionless velocity in radial direction (v^*R/ν)
z	dimensionless axial coordinate (z^*/R)

Greek letters

α	thermal diffusivity (m^2/s)
β	thermal expansion coefficient (1/K)
κ	thermal conductivity (J/(m s K))
μ	viscosity (kg/(m s))
ν	kinematic viscosity (m^2/s)
ρ	density (kg/m^3)
σ	surface tension (N/m)
ϕ	dimensionless stream function ($\phi^*/(Z\nu)$)

Subscript

max	maximum value

Superscript

$*$	dimensional value

diameter [2]. For this reason, we have selected in our model a float-zone configuration that has been used under normal gravity conditions (i.e. about 1 g). In passing, we would like to mention the significance of Marangoni convection in microgravity experiments where the natural convection is reduced to a minimum. In addition, in order to be able to make the Marangoni convection more pronounced in the model, we have deliberately selected certain values for the operating conditions such as temperature gradients and the length of free surface. The purpose of such selection is to be able to study the effect of Marangoni convection effectively under normal gravity conditions.

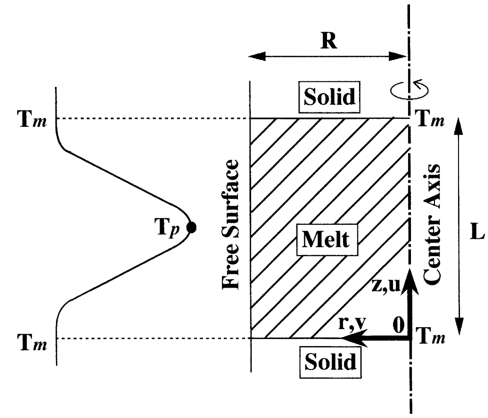

Fig. 1. Basic configuration and coordinate system.

Another way of reducing the intensity of the natural convection in the liquid bridge under normal gravity conditions is the use of a half-zone configuration in the model. In this configuration the liquid bridge is assumed be suspended between an upper flat disk with higher temperature and a lower flat disk with lower temperature. Such a configuration has been widely used for a low temperature liquid [3,4] and for high temperature melt [5] without crystal growth. However, in an actual FZ experiment on Earth the hottest section is located in the middle of the liquid zone [4] as shown in Fig. 1. It would must therefore be better to model the whole liquid zone (the so-called full-zone) for accurate predictions. In such a full-zone configuration, the natural convection is observed in the upper half above the hottest section. It was reported that the interaction of natural and Marangoni convective modes in the liquid zone have affected significantly the flow patterns [6] and flow oscillations [7].

In an actual crystal growth experiment (FZ), the convective flows in the melt and the crystal/melt and melt/feed interfaces are controlled by the rotation of the crucible system. In order to determine the best rotation rate for growing high quality crystals by FZ, a knowledge of the flow velocity distribution in the liquid bridge is essential. This requires a good understanding of relative contributions of natural and Maragoni convections.

In pursuit this goal, one of the authors has previously studied the natural and Marangoni convection modes in a cylindrical liquid bridge using the order of magnitude method [8]. He proposed an evaluating technique for determining the dominant convection mode in the liquid. The order-of-magnitude method is simple and useful for examining the effects of the Marangoni, Grashof and Prandtl numbers on the Reynolds number. However, the proportionality constant cannot be determined by the order-of-magnitude method. Numerical simulations or experimental observations are required to have accurate predictions for the effect of these dimensionless numbers on the flow pattern and the location of the maximum velocity in the liquid [8]. The authors have previously studied the Marangoni convection in a liquid bridge with half-zone configuration under a microgravity field by means of numerical simulation [9]. The Marangoni convection in a liquid bridge with full-zone configuration has also been numerically studied, and the Reynolds number, based on the maximum flow velocity in the liquid due to the Marangoni convection has been correlated with the Marangoni, Prandtl and Biot numbers [10].

In the present study, with the addition of the effect of the Biot number, we study numerically the natural and Marangoni convection modes in a liquid bridge with full-zone configuration. Results are presented in the forms of diagrams for the purpose of predicting the dominant convection. Furthermore, the transient behavior of the convection modes in the liquid for various levels of microgravity is discussed.

2. Model description and numerical procedure

Fig. 1 shows the basic configuration and coordinate system used for the present model. A liquid bridge between two stationary rods with the same radius, R, is heated from the outside surface. The ambient gas temperature profile, $T_a(z)$, is described by the following equation:

$$T_a(z) = T_m + (T_p - T_m)\exp\left\{-25\left(z - \frac{L}{2}\right)^2\right\} \tag{1}$$

The model includes the following assumptions: (i) the fluid is incompressible and Newtonian; (ii) the growth system is axisymmetric and laminar; (iii) the solid/liquid interfaces, which are at T_m, are flat, and no crystal growth or melting occurs; (iv) surface tension of the liquid is very high and the liquid/gas interface is cylindrical; (v) the heat transfer between the liquid bridge and the ambient gas is only through conduction and convection, and the radiative heat transfer can be ignored. Under these assumptions, the dimensionless governing equations are given as follows:

Continuity

$$\frac{\partial u}{\partial z} + \frac{1}{r}\frac{\partial}{\partial r}(rv) = 0 \tag{2}$$

Momentum

$$\frac{\partial u}{\partial t} + u\frac{\partial u}{\partial z} + v\frac{\partial u}{\partial r} = -\frac{\partial p}{\partial z} + \frac{\partial^2 u}{\partial z^2} + \frac{1}{r}\frac{\partial}{\partial r}\left(r\frac{\partial u}{\partial r}\right) + \frac{Gr}{\mathrm{Asp}^3}T \tag{3}$$

$$\frac{\partial v}{\partial t} + u\frac{\partial v}{\partial z} + v\frac{\partial v}{\partial r} = -\frac{\partial p}{\partial r} + \frac{\partial^2 v}{\partial z^2} + \frac{\partial}{\partial r}\left(\frac{1}{r}\frac{\partial}{\partial r}(rv)\right) \tag{4}$$

Energy

$$\frac{\partial T}{\partial t} + u\frac{\partial T}{\partial z} + v\frac{\partial T}{\partial r} = \frac{1}{Pr}\left\{\frac{\partial^2 T}{\partial z^2} + \frac{1}{r}\frac{\partial}{\partial r}\left(r\frac{\partial T}{\partial r}\right)\right\} \tag{5}$$

The dimensionless variables are defined as: $r = r^*/R$, $z = z^*/R$, $t = t^*/(R^2/\nu)$, $u = u^*/(\nu/R)$, $v = v^*/(\nu/R)$, $T = (T^* - T_m)/(T_p - T_m)$, $p = p^*/(\rho\nu^2/R^2)$, where '$*$' is used to denote a dimensional quantity.

Boundary conditions are given as follows:

Along the solid/liquid interfaces ($z = 0$ and Asp)

$$u = v = 0, \quad T = 0 \tag{6}$$

Along the centerline ($r = 0$)

$$\frac{\partial u}{\partial r} = v = 0, \qquad \frac{\partial T}{\partial r} = 0 \tag{7}$$

Along the free surface ($r = 1$)

$$\frac{\partial u}{\partial r} = -\left(\frac{Ma}{\mathrm{Asp}}\right)\frac{\partial T}{\partial z}, \quad v = 0$$

$$\frac{\partial T}{\partial r} = Bi(T_a - T) \tag{8}$$

Eqs. (1)–(8) were discretized by the control volume method on a staggered grid system, and solved by the SIMPLE algorithm [11,12]. Aspect ratio, Asp, was fixed as 2.0 in this study. The numerical domain was divided into 81 (axial) × 61 (radial) control volumes. In order to obtain accurate results, a nonuniform grid arrangement with a small grid spacing near the free surface was used [10]. For the steady state solution, the second-order central and the first-order upwind mixed hybrid scheme were applied to the inertial terms in the governing equations. For the transient solution, the QUICK scheme [13] was used.

3. Results and discussion

3.1. Effect of natural convection

Results of numerical simulations for the stream function and temperature are depicted in Fig. 2a and b for a reduced (10^{-4} g) and normal gravity (1 g) levels. Fig. 2 describes the effect of gravity on the stream function (left half) and isotherms (right half) at the steady state when $Pr = Bi = 1.0$, $Ma = 4 \times 10^3$ and the radius of the liquid bridge is 3.0 mm. Under the reduced gravity field (a), the size of the upper and lower flow cells, both flowing from the center of the free surface to their respective rods along the free surface, are almost identical. On the other hand, under the normal gravity field (b), the upper cell is enhanced by the natural convection while the lower cell was suppressed. The effect of change in gravity levels is obvious. In Fig. 3, the Reynolds number based on the maximum velocity is depicted. In the figure the solid lines represent the following equations:

$$Re_{\max} = 0.0405 BiMa \quad (Re_{\max}Pr < 1) \tag{9}$$

$$Re_{\max} = 0.15\left\{\frac{(BiMa)^2}{Pr}\right\}^{1/3} \quad (Re_{\max}Pr < 1) \tag{10}$$

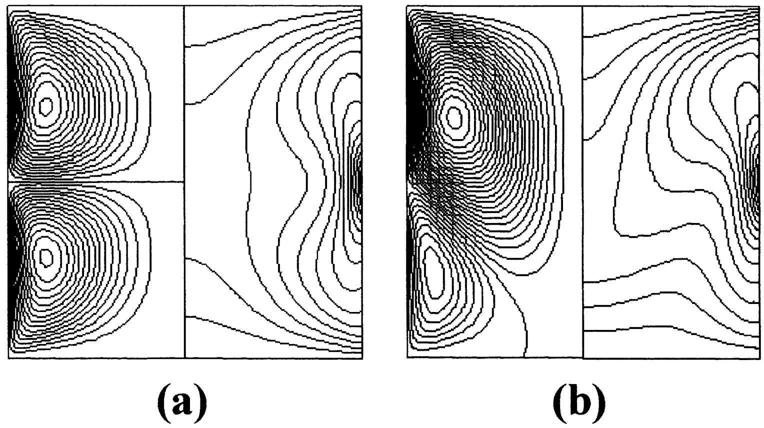

Fig. 2. Effect of gravity on stream function (left half) and isotherms (right half) when $Pr = Bi = 1$, $Ma = 4 \times 10^3$ and radius of the liquid bridge is 3.0 mm. (a) Under reduced gravity, 10^{-4} g, $Gr = 1.6$, and (b) under normal gravity, 1 g, $Gr = 1.6 \times 10^4$.

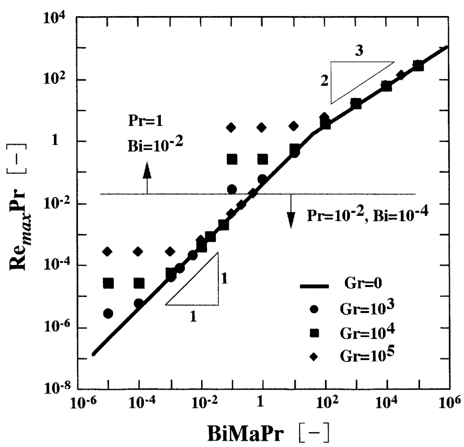

Fig. 3. Effect of natural convection on the maximum Reynolds number.

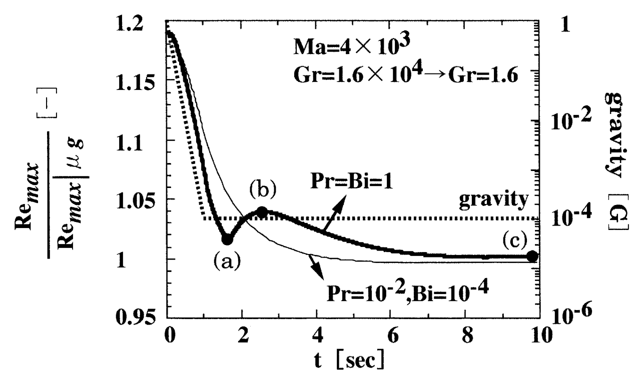

Fig. 5. Transient behavior with varying gravity, from 1 to 10^{-4} g.

Eqs. (9) and (10) were previously obtained by the correlation of numerical results on the Marangoni convection alone in the liquid bridge with full-zone configuration [10]. As shown in Fig. 3, natural convection enhances the maximum Reynolds number, and the curves deviate from Eqs. (9) and (10) when the Grashof number is increased.

3.2. Graphs for evaluation of the dominant convection

Results shown in Fig. 3 are rearranged in Fig. 4, in which (a) and (b) correspond the cases where $Re_{\max}Pr < 1$ and $Re_{\max}Pr > 1$, respectively. In this graphical representation, when the Marangoni convection is dominant in the liquid, the graphs exhibit a linear relationship with a slope of unity.

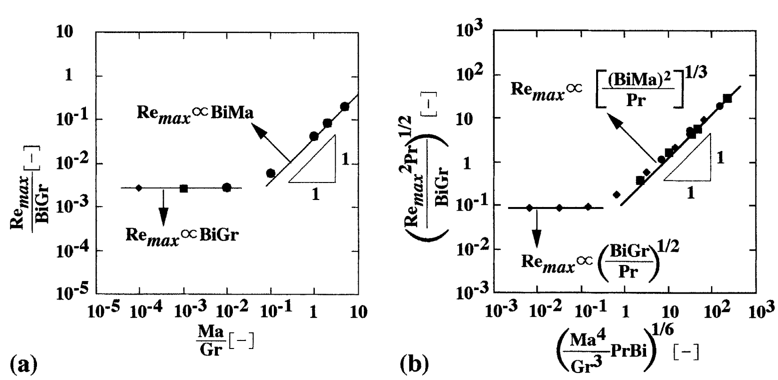

Fig. 4. Diagrams for the estimation of dominant convection: (a) for $Re_{\max}Pr < 1$, and (b) for $Re_{\max}Pr > 1$.

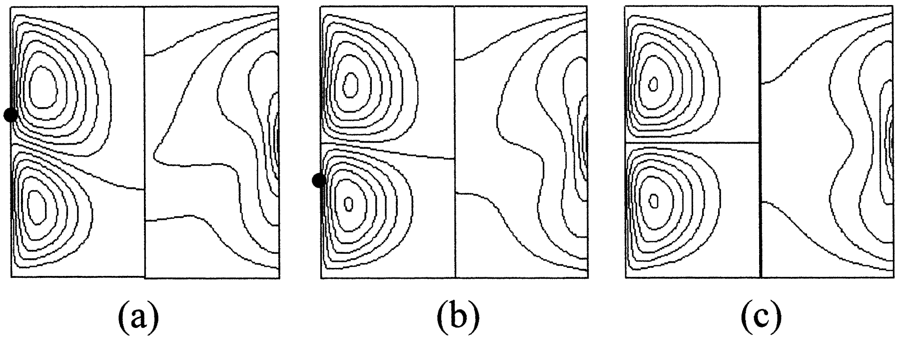

Fig. 6. Flow (left half) and temperature (right half) fields when $Pr = Bi = 1$ during gravity change. (a) 1.6; (b) 2.5 and (c) 10 s.

This corresponds to the following relationships:

$$Re_{\max} \propto BiMa \quad (Re_{\max}Pr < 1) \tag{11}$$

$$Re_{\max} \propto \left\{\frac{(BiMa)^2}{Pr}\right\}^{1/3} \quad (Re_{\max}Pr > 1) \tag{12}$$

On the other hand, the absisca is shown constant when natural convection is dominant in the liquid. This translates into the following relationships:

$$Re_{\max} = 2.61 \times 10^{-3}\, BiGr \quad (Re_{\max}Pr < 1) \tag{13}$$

$$Re_{\max} = 0.0831\, (BiGr/Pr)^{1/2} \quad (Re_{\max}Pr > 1) \tag{14}$$

Thus, by representing the results in the format suggested in Fig. 4, the dominant convection in the liquid bridge with full-zone configuration can readily be determined. However, the proportionality constants in Eqs. (9), (10), (13) and (14) must be affected by the shapes of liquid/gas and solid/liquid interfaces. As the authors have previously reported, swelling of the interface leads to a faster flow velocity [14]. The effect of the interface shapes should be examined in future works.

3.3. Transient behavior of convection under varying gravitational field

The interest of studying the transient behavior of the convective flow in the liquid bridge in FZ systems from the fact that there have been a number of crystal growth experiments using some inexpensive microgravity environments such as drop towers and parabolic flights. One of the goals of crystal growth experiments in these environments is the investigation of Marangoni convection. In such experiments, the gravity level changes from 1 g to a microgravity in a very short period of time. It is important to examine the effect of such a sudden change in the gravity level on the flow modes in FZ. Fig. 5 presents the result of our numerical simulation for the transient behaviors of the convection modes in the liquid bridge with full-zone configuration. In the figure, a broken line represents the variation of gravity level. The gravitational constant was changed from 1 to 10^{-4} g in 1 s. A thinner line describes the variation of the maximum Reynolds number normalized by the value at $Gr = 0$ when $Pr = 10^{-2}$ and $Bi = 10^{-4}$, which corresponds to a semiconductor melt. A bold line shows the case of $Pr = Bi = 1$, which corresponds to an oxide melt. The maximum Reynolds number decreases as the gravity decreases because of suppression of the natural convection, and continues to decrease even the gravitational level stays at 10^{-4} g. In the case of liquid with $Pr = 10^{-2}$ and $Bi = 10^{-4}$, the maximum Reynolds number decreases monotonously. On the other hand, in the case of a liquid with $Pr = Bi = 1$, the maximum Reynolds number reaches a local maximum at about 2 s, and then decreases again. Fig. 6 shows flow and temperature fields when $Pr = Bi = 1$. Fig. 6a–c describe the stream functions and isotherms at the corresponding times that are marked in Fig. 5. The "●" symbols in Fig. 6 represent the position of the maximum velocity. As shown in Fig. 6, the position of the maximum velocity moves from the upper to the lower cell as natural convection is suppressed.

4. Conclusion

Natural and Marangoni convection modes in a liquid bridge with full-zone configuration were numerically studied, and the following results were obtained:

1. The natural convection in the liquid zone was enhanced in the upper section of the zone while it was suppressed in the lower section of the zone.
2. Results of numerical simulation were presented in graphical forms, and new graphs were proposed for purpose of evaluating the dominant convection in the liquid, including the Biot number. These graphs provide essential information for determining experimental conditions in the liquid during crystal growth by the floating zone, and also for investigating the Marangoni convection under normal gravity conditions.
3. Transient behavior of natural convection under varying gravity fields depends on the physical properties of the liquid. Even the gravity level is kept at a constant microgravity value, the level of convection in the liquid still

varies, and it takes a period of time before the system reaches a steady state.

References

[1] A. Bohm, A. Ludge, W. Schroder, in: D.J.T. Hurle (Ed.), Handbook of Crystal Growth, Vol. 2a, North-Holland, Amsterdam, 1994 (Chapter 4).
[2] P. Dold, A. Croll, K.W. Benz, J. Cryst. Growth 183 (1998) 545.
[3] H.C. Kuhlmann, Thermocapillary Convection in Models of Crystal Growth, Springer Tracts in Modern Physics, Vol. 152, Springer, Berlin, 1999.
[4] Ch.H. Chun, J. Cryst. Growth 48 (1980) 600.
[5] S. Nakamura, T. Hibiya, K. Kakimoto, N. Imaishi, S. Nisizawa, A. Hirata, K. Mukai, S. Yoda, T. Morita, J. Cryst. Growth 186 (1998) 85.
[6] W. Shyy, M.-H. Chen, J. Cryst. Growth 108 (1991) 247.
[7] T. Suzumura, S. Umemura, Y. Okano, J. Jpn. Assoc. Cryst. Growth (in Japanese) 27 (2000) 76.
[8] Y. Okano, A. Hatano, A. Hirata, J. Chem. Eng. Jpn. 22 (1989) 385.
[9] Y. Okano, S. Kunikata, T. Fujioka, S. Sakai, M. Koyama, Numer. Heat Transfer, Part A 31 (1997) 407.
[10] Y. Okano, S. Kunikata, S. Sakai, T. Fujioka, A. Hirata, M. Sakurai, M. Koyama, T. Morita, in: S.N. Atluri, G. Yagawa (Eds.), Advances in Computational Engineering Science, Tech Science Press, 1997, p. 232.
[11] S.V. Patankar, Numerical Heat Transfer and Fluid Flow, Hemisphere, London, 1980.
[12] A. Nakayama, PC-Aided Numerical Heat Transfer and Convective Flow, CRC Press, Boca Raton, 1995.
[13] B.P. Lenard, Compt. Methods Appl. Mech. Eng. 19 (1979) 59.
[14] Y. Okano, N. Audet, S. Dost, S. Kunikata, J. Cryst. Growth 204 (1999) 243.